

## Interbilayer interactions from high-resolution x-ray scattering

Horia I. Petrache,<sup>1,\*</sup> Nikolai Gouliarov,<sup>1</sup> Stephanie Tristram-Nagle,<sup>2</sup> Ruitian Zhang,<sup>1,†</sup> Robert M. Suter,<sup>1</sup> and John F. Nagle<sup>1,2,‡</sup>

<sup>1</sup>Department of Physics, Carnegie Mellon University, Pittsburgh, Pennsylvania 15213

<sup>2</sup>Department of Biological Sciences, Carnegie Mellon University, Pittsburgh, Pennsylvania 15213

(Received 25 November 1997)

The fundamental issue of interactions between lipid bilayers is addressed experimentally and theoretically. We report high-resolution x-ray scattering data for bilayers composed of three different kinds of phosphatidylcholine lipids. These data yield the interbilayer water spacing fluctuation  $\sigma$ , as well as the traditional osmotic pressure  $P$ , both as functions of the lamellar repeat spacing  $D$  and the aqueous separation  $a$ . We show theoretically how to obtain the functional form of the fluctuational free energy from the  $\sigma$  data, which is then determined to within a factor that depends upon the bending modulus,  $K_c$ . The resulting functional form determined from experimental data has an exponential decay rather than the power law decay that applies for hard confinement in the large  $a$  regime, thereby showing that a theory of soft confinement is necessary. However, the existing theory of soft confinement predicts an exponential decay, but with a smaller decay length  $\lambda_{fl}$  than we obtain. We then use these results to analyze the osmotic pressure data in terms of the bending modulus  $K_c$  and the interbilayer interactions consisting of van der Waals and hydration interactions. For all three chemically different lipids we find that the decay length  $\lambda$  of the hydration pressure is 1.9–2.0 Å; the Hamaker parameter for the van der Waals interaction is about  $5 \times 10^{-14}$  erg if the bending moduli  $K_c$  are chosen to be different for the three lipids and in the range  $(0.5-0.8) \times 10^{-12}$  erg. [S1063-651X(98)11606-9]

PACS number(s): 87.22.Bt, 87.64.Bx, 87.15.Kg, 61.30.-v

### I. INTRODUCTION

A major goal in biophysics is to describe and understand the basic interactions between macromolecular structures. One of the more important examples is the interaction between two membranes; such interactions are involved in biologically essential membrane fusion processes [1] as well as in maintaining the organization of membrane stacking in myelin, retinal rods [2], and chloroplast thylakoid disks [3]. Each type of biomembrane is a complex multicomponent mixture that includes a particular set of specialized proteins that may mediate particular intermembrane interactions. However, the structural basis of each biomembrane is a lipid bilayer and interbilayer interactions, though only a subset of general intermembrane interactions, already pose interesting issues for those macromolecular interactions that are the focus of this paper.

When lipids are mixed with water, they often form smectic liquid crystals. On a scale of order  $10^2-10^3$  Å the structure can be thought of as bilayers stacked in a direction perpendicular to the bilayers, as shown in Fig. 1. On the scale of  $10 \mu\text{m}$  the structures may consist, for the simplest sample preparations, of multilamellar vesicles that are globally isotropic and give rise to powder pattern x-ray scattering. Various sample preparation procedures also yield oriented lipid bilayers [4] so that there is a common macroscopic director. The focus of this paper is on the interactions that determine

the lamellar repeat spacing  $D$  in Fig. 1 and, more specifically, the water spacing, defined variously as  $D_w$  or  $D'_w$  (*vide infra*). This paper will not be concerned with the problem of self-assembly of the bilayers; rather, a smectic structure will be assumed to arise from much stronger hydrophobic energies that separate the oily chains from the water and the hydrophilic energies that keep the headgroups in an aqueous environment.

Although interbilayer interactions are ultimately all elec-

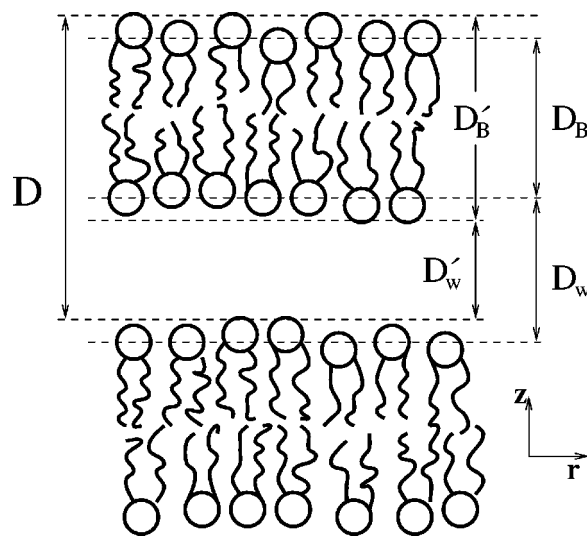


FIG. 1. Sketch of two neighboring bilayers. The size of the interbilayer water space is defined as either  $D_w$  or  $D'_w$ . The respective bilayer thicknesses, indicated by subscript  $B$ , satisfy  $D_B + D'_B = D = D'_B + D'_w$ , where  $D$  is the repeat spacing for a stack of bilayers.

\*Electronic address: hp28@andrew.cmu.edu

†Present address: Chemistry Division, Argonne National Lab, Argonne, IL 60439.

‡Electronic address: nagle@andrew.cmu.edu

tromagnetic from the point of view of traditional physics, this simplistic description is totally inadequate to understand biophysical systems [5]. Rather, the total interaction is better comprehended as involving several contributions. For lipid bilayers the first contribution is a long range attractive van der Waals interaction that accounts for the fact that many bilayer systems do not swell indefinitely as water is added. Instead, the  $D$  repeat spacing in Fig. 1 reaches a limiting value,  $D_0$ , and additional water then forms a separate thermodynamic phase that contains only a small concentration of monomeric lipid molecules [6]. When  $D=D_0$ , the system is said to be fully hydrated.

A nonzero water spacing  $D_W$  implies the existence of some repulsive force to balance the van der Waals attractive force. Rand, Parsegian and co-workers developed a technique that applies osmotic pressure  $P$  to shrink  $D$  and  $D_W$  [7]. The  $P(D)$  data have been interpreted as indicating an exponentially decaying repulsive force that has been called the hydration force [7,8]. Theories [9,10] have been presented for the hydration force, but it remains an outstanding topic of fundamental interest and much uncertainty [11].

In this paper we will accept the working hypothesis that there is a separable hydration interaction with an exponential decay. Adding this to the van der Waals interaction yields an interaction energy per unit area  $V(z)$  of two bilayers with a fluctuating water spacing  $z$  between them,

$$V(z) = P_h \lambda e^{-z/\lambda} - \frac{H}{12\pi} U_{\text{vdW}}(z). \quad (1)$$

The functional dependence of the van der Waals contribution is

$$U_{\text{vdW}}(z) = \left( \frac{1}{z^2} - \frac{2}{(z+D_B)^2} + \frac{1}{(z+2D_B)^2} \right), \quad (2)$$

where  $D_B$  is the bilayer thickness. For the kind of bilayers studied in this paper, the Hamaker parameter  $H$  has been estimated to lie in the range  $10^{-14} - 10^{-13}$  erg [5,7,12,13]. From  $P(D)$  measurements  $\lambda$  has been estimated to be in the range 1.3–2.1 Å [7,12]. The numerical value of  $P_h$  is tightly coupled to whether one chooses the water spacing  $z$  to be  $D_W$  or  $D'_W$  in Fig. 1. Using the  $D'_W$  convention yields  $P_h = 5 \times 10^8$  ergs/cm<sup>3</sup> [14] and using the  $D_W$  convention just rescales  $P_h$  by  $\exp[(D_W - D'_W)/\lambda]$ ; this is clearly not an essential difference. In this paper we will use the simpler symbol  $a$  to denote the average water spacing and  $z$  to denote the instantaneous, local water spacing. More importantly, the values for  $P_h$ ,  $\lambda$ , and  $H$  for multilamellar systems have been obtained from experiment using simple theories that are continuing to evolve [15]. One goal of the present research is to test these fundamental interactions experimentally and to obtain more reliable estimates of the parameters.

As Helfrich showed [16], there is another important repulsive force when the bilayers are flexible, as in the biologically relevant thermodynamic phase that is variously called fluid,  $L_\alpha$  or smectic  $A$ , so that undulation and compression modes play a role. This force is due to the increased free energy from the decrease in entropy that accompanies the reduction of out-of-plane fluctuations; such reduction is re-

quired when the water spacing is reduced. Helfrich analyzed this effective force in the case when there are no van der Waals or hydration interactions, only the steric interactions caused by collision of bilayers. In this case, Helfrich showed [16] that the steric free energy per unit area has the form

$$f_U = 0.42 \frac{(k_B T)^2}{K_c a^2}, \quad (3)$$

where  $K_c$  is the bending modulus, which has been measured on single bilayers to be in the range  $(0.5 - 2) \times 10^{-12}$  erg [17–20].

When one has a repulsive hydration force, the confinement of each membrane is softer than for purely steric interactions. In this case, it has been proposed [15,21] that the undulation interaction free energy in Eq. (3) should be modified and a formula involving an exponential with decay length  $2\lambda$ ,

$$f_{U2} = (\pi k_B T / 16) (P_h / K_c \lambda)^{1/2} \exp(-a/2\lambda), \quad (4)$$

has been offered [22]. In a more recent and fuller theory due to Podgornik and Parsegian [15] Eq. (4) again appears. However, the theory was then extended to include van der Waals interactions and then it is not clear if Eq. (4) remains valid. One achievement of the present paper is to employ experimental data to determine the functional form for this interaction.

It has also been shown on the basis of  $P(D)$  data [14] that there is an additional repulsive interaction at small distances that was described as the beginning of a steric interaction between head groups and an extra exponential has been used to fit the  $P(D)$  data [12] for large  $P$  and water spacing  $a$  smaller than 4 Å. Our data do not go to such small water spacings or such high pressures, so this additional force will not be considered further in this paper.

From  $P(D)$  data for flexible egg PC bilayers in the  $L_\alpha$  phase McIntosh and Simon [12] suggested that the hydration force is dominant for water spacings from 4 to 8 Å and their fits gave  $\lambda = 1.38$  Å and  $P_h = 4 \times 10^8$  dyn/cm<sup>2</sup>. Their data, and especially their perceptive comparisons of the undulatory  $L_\alpha$  phase with the less flexible gel and subgel phases, indicated that the undulation interaction dominates the hydration interaction from 8 Å to nearly the equilibrium water spacing  $a_0$  of about 15.4 Å at full hydration and  $P=0$ , where, of course, the attractive van der Waals force plays a coequal role. It was clear from those results [12] that there are several different kinds of repulsive interactions, which involve a number of different phenomenological parameters. As was appreciated by McIntosh and Simon [12],  $P(D)$  data are not sufficient to determine uniquely all the interaction parameters, and they proceeded by choosing estimates  $H = 2.5 \times 10^{-14}$  erg and  $K_c = 10^{-12}$  erg based on experiments on other model systems. Using Eq. (4), the  $P(D)$  data were then satisfactorily fit, but this was not, of course, confirmation of Eq. (4) or of the values of the parameters  $H$  and  $K_c$ .

Our innovation is to supplement  $P(D)$  data with data for the root mean square fluctuations  $\sigma(D)$  in the water spacing. This innovation opens a second window into lipid bilayer interactions in the soft confinement regime. Obtaining  $\sigma$  also requires theoretical interpretation of x-ray scattering data.

The theory we use is an improved version [23] of the Caille [24] theory of scattering from a model of smectic liquid crystals [25]. This theory contains  $K_c$  and a bulk modulus  $B$  for compression. This bulk modulus  $B$  provides a phenomenological, harmonic approximation to the more fundamental hydration force and van der Waals forces.

The paper is organized as follows. In Sec. II A the Caille smectic theory of scattering and the thermodynamic theory of smectic liquid crystals are reviewed to show how the undulation free energy can be derived from the experimentally determined Caille  $\eta_1$  parameter. The theoretical analysis is extended in Sec. II B to relate the conventional smectic theory to the underlying fundamental interbilayer interactions. This analysis leads to a new way to interpret conventional osmotic pressure data that uses  $\sigma(D)$  data to obtain experimental information about the fluctuation pressure. Our data are presented in Sec. III for three lipids. In Sec. IV the results of fitting the data to the theory are presented.

## II. THEORY

### A. Review of standard smectic liquid crystal theory

Analysis of high-resolution x-ray data [26,27] using the Caille scattering theory [23,24] yields the interbilayer fluctuation  $\sigma$  as will now be shown. The Caille theory is derived from a continuum harmonic smectic liquid crystal potential [25]

$$H_c = \int dx \int dy \int dz \left[ \frac{1}{2} K \left( \frac{\partial^2 u}{\partial x^2} + \frac{\partial^2 u}{\partial y^2} \right)^2 + \frac{1}{2} B_3 \left( \frac{\partial u}{\partial z} \right)^2 \right], \quad (5)$$

where the fundamental variable  $u = u(x, y, z)$  gives bilayer fluctuations along  $z$ , perpendicular to the bilayer, from the mean equilibrium position. The first term on the right hand side of Eq. (5) accounts for the energy to bend bilayers. The last term accounts for the energy of interaction between adjacent bilayers in the harmonic approximation. We will postpone to the next subsection the important issue of how this compression term is related to the fundamental interactions  $V(z)$  in Eq. (1). Instead, we emphasize that the compression term in Eq. (5) assumes a continuum model instead of having discrete bilayers. Therefore, Eq. (5) may be made more realistic by replacing the continuum derivatives in the  $z$  direction by finite differences [28,29]

$$H_d = \int dx \int dy \left[ \sum_{n=0}^{N-1} \frac{1}{2} K_c \left( \frac{\partial^2 u_n}{\partial x^2} + \frac{\partial^2 u_n}{\partial y^2} \right)^2 + \sum_{n=0}^{N-1} \frac{1}{2} B(u_{n+1} - u_n)^2 \right], \quad (6)$$

where the parameters in Eqs. (5) and (6) are related by  $B = B_3/D$  and  $K_c = KD$ , where  $K_c$  is the usual bending modulus. We will call Eq. (6) the discrete smectic theory and Eq. (5) the continuum smectic theory. We have performed numerical calculations, following [23], that show that there is practically no difference in predicted x-ray line shapes for

the two theories. In both theories the power law tails in the scattering peaks are governed by the Caille  $\eta_1$  parameter defined by

$$\eta_1 = \frac{k_B T}{8 \sqrt{B K_c}} \frac{4\pi}{D^2}. \quad (7)$$

Derivations of properties of smectic theories have been performed many times, but we present it again here with special care for the numerical factors that are essential for detailed analysis of data. Results will be given for both continuum and discrete models, but we only give the derivation for the discrete smectic theory given by Eq. (6) because it is the better physical model that is more directly related to the fundamental interactions in Eq. (1). As usual, consider the Fourier representation of the displacement variables,

$$u(x, y, n) = \sum_{Q_x, Q_y, Q_z} U(Q_x, Q_y, Q_z) e^{i\vec{Q} \cdot \vec{R}}, \quad (8)$$

with  $\vec{R} = \vec{r} + nD\hat{z}$  and the vectors  $\vec{Q}$  taking values in the first Brillouin zone defined by the in-plane molecular size for  $Q_x, Q_y$ , and by the membrane spacing  $D$  for  $Q_z$ . In terms of independent variables,  $H_d$  is written as

$$H_d = \sum_{\vec{Q}} \frac{1}{2} h_{\vec{Q}} |U_{\vec{Q}}|^2 = \sum_{\vec{Q}, Q_z > 0} h_{\vec{Q}} |U_{\vec{Q}}|^2, \quad (9)$$

where

$$h_{\vec{Q}} = NL^2 [K_c Q_r^4 + 4B \sin^2(Q_z D/2)]. \quad (10)$$

From the equipartition theorem, the mode amplitude is

$$\langle |U_{\vec{Q}}|^2 \rangle = k_B T / h_{\vec{Q}}. \quad (11)$$

The partition function is given by

$$Z = \prod_{\vec{Q}, Q_z > 0} \int C d(\text{Re} U_{\vec{Q}}) d(\text{Im} U_{\vec{Q}}) e^{-\beta H_d}, \quad (12)$$

where the constant  $C$  has the role of making  $Z$  dimensionless by compensating for a unit of  $(\text{length})^{-2}$  for each mode  $\vec{Q}$ . The integration yields

$$\begin{aligned} Z &= \prod_{\vec{Q}, Q_z > 0} C \int_{-\infty}^{\infty} d(\text{Re} U_{\vec{Q}}) e^{-\beta h_{\vec{Q}} (\text{Re} U_{\vec{Q}})^2} \\ &\quad \times \int_{-\infty}^{\infty} d(\text{Im} U_{\vec{Q}}) e^{-\beta h_{\vec{Q}} (\text{Im} U_{\vec{Q}})^2} \\ &= \prod_{\vec{Q}, Q_z > 0} C \frac{\pi}{\beta h_{\vec{Q}}}. \end{aligned} \quad (13)$$

Then, the free energy is

$$F = -\frac{1}{\beta} \ln Z = \frac{k_B T}{2} \sum_{\text{all } \vec{Q}} \ln \left( \frac{\beta h_{\vec{Q}}}{C \pi} \right) = \sum_{\text{all } Q_z} F(Q_z), \quad (14)$$

with the free energy per compression mode  $F(Q_z)$  given by

$$F(Q_z) = \frac{k_B T}{2} \left( \frac{L}{2\pi} \right)^2 \int_{\vec{Q}_r} d^2 Q_r \ln \left( \frac{\beta h \vec{Q}}{C \pi} \right). \quad (15)$$

The free energy of interest is the difference from a reference state with  $B=0$ ,

$$\Delta F = F(B \neq 0) - F(B=0), \quad (16)$$

given by

$$\frac{\Delta F}{L^2} = \sum_{\text{all } Q_z} \frac{\Delta F(Q_z)}{L^2} = \frac{k_B T}{8} D \sqrt{\frac{B}{K_c}} \sum_{\text{all } Q_z} |2 \sin(Q_z D/2)|. \quad (17)$$

Summing over  $\vec{Q}_z$  and converting to the free energy per unit area of one bilayer yields

$$\frac{\Delta F_{\text{fl}}}{N L^2} = \frac{4}{\pi} \frac{k_B T}{8} \sqrt{\frac{B}{K_c}}, \quad (18)$$

where the subscript fl has been added to emphasize that this is only the fluctuational contribution to the free energy, as will be discussed in the next subsection.

The mean square fluctuation in the water spacing  $a$  for the discrete smectic theory is given by

$$\begin{aligned} \sigma^2 &= \langle [u(x, y, n+1) - u(x, y, n)]^2 \rangle \\ &= k_B T \sum_{Q_z} \sum_{Q_r} \frac{4 \sin^2(Q_z D/2)}{N L^2 [K_c Q_r^4 + 4B \sin^2(Q_z D/2)} \\ &= \frac{k_B T}{8} \frac{1}{\sqrt{K_c B}} \frac{2}{N} \sum_{Q_z} \left| \sin \left( \frac{Q_z D}{2} \right) \right| = \frac{4}{\pi} \frac{k_B T}{8} \frac{1}{\sqrt{K_c B}}. \end{aligned} \quad (19)$$

Comparing Eq. (19) to Eq. (7) gives

$$\sigma^2 = \eta_1 D^2 / \pi^2. \quad (20)$$

It should be noted that, despite this close connection between the Caille scattering parameter  $\eta_1$  and the fluctuation  $\sigma$  in nearest neighbor distance  $a$ , it is the long range correlations and not the nearest neighbor correlations that give the power law tails in the x-ray scattering peaks.

A similar derivation for the free energy of the continuum smectic theory yields a factor of  $\pi/2$  instead of the factor of  $4/\pi$  in Eq. (18). For  $\sigma^2$  the numerical factor for the continuum smectic theory depends upon a delicate interpretation of how the correlation function should be defined; it has been suggested [27] that the numerical factor  $4/\pi$  in Eq. (19) should be replaced by 1.09, but we now tend to prefer replacing it with  $\pi/2$ , just as in Eq. (18). However, this latter difference regarding the best equation for  $\sigma^2$  for the continuum potential is a moot point, since the discrete form of the model is clearly more physical.

### B. Extension to fundamental interactions

Let us now return to the problem of relating the usual smectic theory embodied in Eq. (6) to fundamental interbi-

layer interactions, such as the putative ones in Eq. (1). Not making the harmonic approximation yields the more realistic potential  $H_R$  defined as

$$H_R = \int dx \int dy \sum_{n=0}^{N-1} \left[ \frac{1}{2} K_c \left( \frac{\partial^2 u_n}{\partial x^2} + \frac{\partial^2 u_n}{\partial y^2} \right)^2 + V(w_n) \right], \quad (21)$$

where  $V$  is a potential such as the one suggested in Eq. (1), the instantaneous spacing between membrane pairs  $n$  and  $n+1$  is  $w_n = a + u_{n+1} - u_n$ ,  $a$  is the average equilibrium water spacing that generally depends upon applied osmotic pressure, and  $u_n$  remains the fluctuation in the  $z$  direction of the  $n$ th membrane from its equilibrium position. Let us expand the bare potential  $V(w)$  to second order about its value at  $a$ ,

$$\begin{aligned} V(w_n) &= V(a) + (dV/dw_n)_a (u_{n+1} - u_n) \\ &\quad + (d^2V/dw_n^2)_a (u_{n+1} - u_n)^2/2. \end{aligned} \quad (22)$$

The first order term vanishes after summation in Eq. (22) for periodic boundary conditions. The second order term clearly contributes to (but is not identical to, *vide infra*) the harmonic  $B$  term in Eq. (6). The leading term  $V(a)$  is the term that is not included in Eq. (6). This means that the free energy given in Eq. (18) only includes the fluctuational contribution. Correcting Eq. (18) for this yields the total free energy in the harmonic approximation

$$\frac{\Delta F}{N L^2} = \frac{4}{\pi} \frac{k_B T}{8} \sqrt{\frac{B}{K_c}} + V(a). \quad (23)$$

From the total free energy, the total osmotic pressure  $P_{\text{osm}}$  can be obtained by taking the negative of the derivative with respect to  $a$ . It is convenient to write this explicitly as

$$P = P_{\text{fl}} + P_{\text{bare}}, \quad (24)$$

where  $P_{\text{bare}} = -dV/da$  and the fluctuational pressure  $P_{\text{fl}}$  derives from the first term on the right hand side of Eq. (23).

It is important to appreciate the implicit complexity of Eqs. (23) and (24) when fluctuational forces are included. This complexity is centered in the phenomenological compression modulus  $B$ . If one is given the water spacing  $a$  and the bare potential, then  $P_{\text{bare}}$  is easy to calculate, but obtaining  $P_{\text{fl}}$  requires knowing  $B$  and its dependence upon  $a$ . Determining  $B$ , in turn, requires knowing all the forces, including the fluctuational force itself. Resolving this theoretically requires some self-consistency condition, such as that used by Podgornik and Parsegian [15]. We do not do that in this paper. Instead, we take an experimental approach.

Because we have experimental data for  $\eta_1$ , we can eliminate  $B$  from Eq. (23) using Eqs. (7) and (20). We then have

$$F_{\text{fl}} = \left( \frac{4}{\pi} \frac{k_B T}{8} \right)^2 \frac{1}{K_c \sigma^2} \quad (25)$$

and

$$P_{\text{fl}} = - \left( \frac{4}{\pi} \frac{k_B T}{8} \right)^2 \frac{1}{K_c} \frac{d\sigma^{-2}}{da}, \quad (26)$$

which allows us to obtain the functional form of the fluctuational pressure straight from data. Furthermore, the actual magnitude of  $P_{fl}$  then follows if  $K_c$  is known. One may know or determine  $K_c$  from other experiments [17–20] or one can use it as a fitting parameter along with the parameters that describe the bare potential in order to fit the measured osmotic pressure. The latter strategy is the one that we shall employ in this paper to evaluate interbilayer interactions.

### III. DATA

Experimental data for DPPC at 50 °C in the  $L_\alpha$  (fluid) phase have been previously reported [26,27] and to this we add data for DMPC and egg PC (EPC) both at 30 °C and both in the  $L_\alpha$  phase. All these lipids have the same glyceryl backbone and PC (phosphatidylcholine) headgroup; egg PC has unsaturated hydrocarbon chains in contrast to the saturated chains in DMPC (14 carbons/chain) and in DPPC (16 carbons/chain). Different hydration levels were produced using the established technique of applying osmotic pressure  $P$  by adding an immiscible polymer, PVP (polyvinylpyrrolidone, MW 40 000) in our studies, to bulk water [7]. The PVP polymer weight concentration was converted into pressure using the procedure of McIntosh and Simon [30]. By varying concentration of PVP the osmotic pressure spanned the range from  $P=0$  to  $P=58$  atmospheres.

Figure 2 shows our osmotic pressure data versus  $D$  space for three lipids. The error in measuring  $D$  was about 0.01 Å. The greatest error in Fig. 2 is in the osmotic pressure due to the difficulty of preparing small samples with precise polymer concentrations. However, the scatter in the  $\ln P$  data is comparable to data reported in the literature [12,7]. We also noticed systematic deviations in  $\ln P$  in samples prepared on two separate occasions, as indicated for DMPC in Fig. 2 by the solid versus open symbols. Uncertainties in  $\ln P$  for the earlier DMPC and the DPPC data were estimated as 0.3, and as 0.2 for the later DMPC data and the EPC data. Another source of error is revealed in the spacings  $D_0$  for fully hydrated samples with no PVP ( $P=0$ ); the variations in  $D_0$  were substantially larger than the measuring error of 0.01 Å. The values of  $D_0$  are indicated in Fig. 2 by arrows. The sum of the squares of the residuals used in fitting theory to the data will include the square residual of  $D_0$  weighted by  $\Delta D_0^{-2}$ .

To obtain the mean square fluctuation in the water spacing between bilayers  $\sigma(D)$ , fully resolved x-ray line shapes were obtained using a silicon analyzer crystal and synchrotron radiation at CHESS as described previously [27]. The data were analyzed following the method of Zhang *et al.* [23]. A typical fit is shown in Fig. 3. The Caille [24] x-ray line shape parameter  $\eta_1$  was converted to  $\sigma$  using Eq. (20). The results are shown in Fig. 4.

To test the theories of interactions it is necessary to convert  $D$  into the water spacing. This conversion involves three considerations. The first consideration is that two definitions of water spacing have been used as shown in Fig. 1. We employ the definition  $a = D'_W$  that is similar to the one used by McIntosh and Simon [14]. This choice of convention makes no difference for the two interactions that turn out to be exponential. It reduces our estimate of the Hamaker parameter  $H$ , but this convention makes only a small difference for the functional form of the van der Waals interaction,

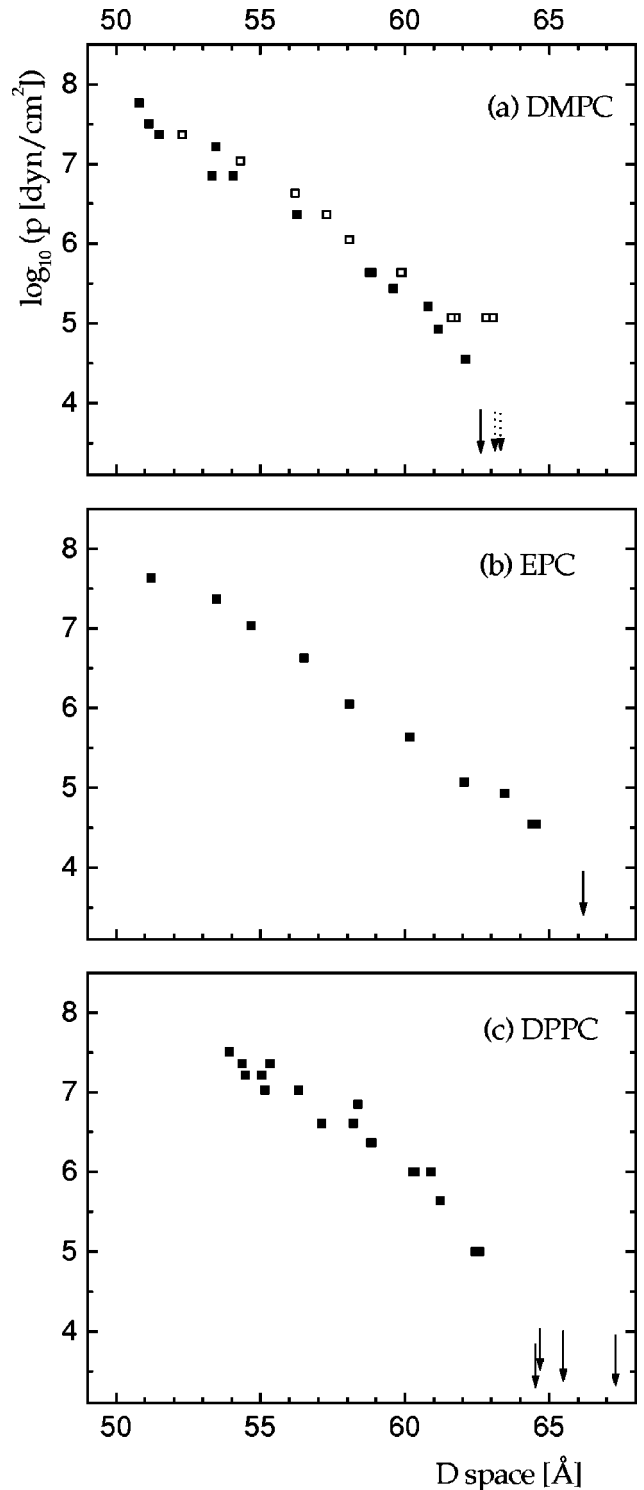


FIG. 2.  $\log_{10}(\text{osmotic pressure})$  vs lamellar repeat  $D$  for (a) DMPC (30 °C), (b) EPC (30 °C), and (c) DPPC (50 °C). In (a) the solid symbols show data for our most recent, most carefully prepared samples and the open symbols show earlier data. The arrows indicate  $D_0$  for  $P=0$ .

since  $D'_W$  is comfortably larger than zero.

The second consideration in obtaining  $a$  is that it is not easy to obtain a reliable partitioning of  $D$  into  $D'_B$  and  $a$ . We have recently accomplished this for DPPC by constructing electron density profiles using the form factors corrected for fluctuations. The maxima in the electron density profiles are

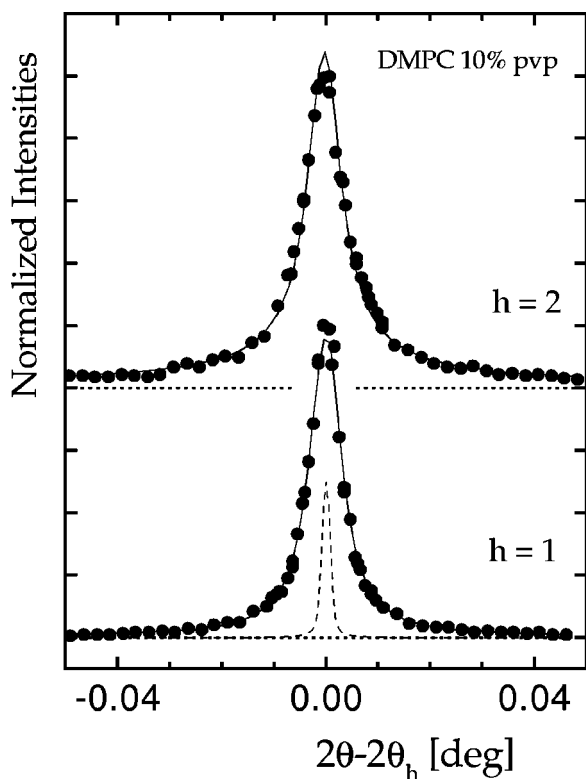


FIG. 3. Normalized data (circles) for two orders,  $h=1$  and  $h=2$ , for DMPC with 10% PVP. Solid curves are fits to the data using modified Caille theory [23]. The instrumental resolution is shown by a dashed curve and the baselines are indicated by dotted lines. For  $h=1$ ,  $\theta_1=1.1844$  corresponding to  $D=58.78\pm 0.01$  Å.

due to the phosphate group and so the distance  $X_{HH}$  between maxima is a relative measure of the bilayer thickness. By comparing the electron density profiles for the gel phase with the  $L_\alpha$  phase, we found [26]  $D'_B=45.2$  Å in the fluid phase of DPPC at full hydration ( $P=0$ ). The most uncertain aspect of this determination was the estimate for the thickness  $D_H$  of the headgroup region. We have since revised our estimate of  $D_H$  from 8 to 9 Å and this increases  $D'_B$  to 47.2 Å. The corresponding determination has not yet been performed for DMPC, and EPC does not form a gel phase. To obtain  $D'_B$  for DMPC and EPC we have instead compared their electron density profiles with that of DPPC, all in the  $L_\alpha$  phase. Since all three lipids in this study have the same phosphatidylcholine headgroup, differences in  $X_{HH}$  should be primarily equal to differences in the thickness of the hydrocarbon chain region. The values of  $X_{HH}$  and the corresponding values of  $D'_B$  are shown in Table I. The  $X_{HH}$  for DMPC is 3.2 Å less than for DPPC. This difference is consistent with the fact that there are two fewer  $\text{CH}_2$  groups per hydrocarbon chain in DMPC and with the NMR order parameters that indicate that the length along the bilayer normal of a  $\text{CH}_2$  group in the plateau region is 0.8 Å [31]. This latter consistency for DMPC lends confidence to our determination for EPC. Table I also shows the corresponding water spacing  $a_0$  for fully hydrated samples. The large range quoted for DPPC reflects the range of  $D_0$  spacings.

The third consideration in obtaining  $a$  is that osmotic pressure should not only squeeze the membranes together by reducing  $a$ , it may also reduce the area/lipid  $A$  [7]. Since

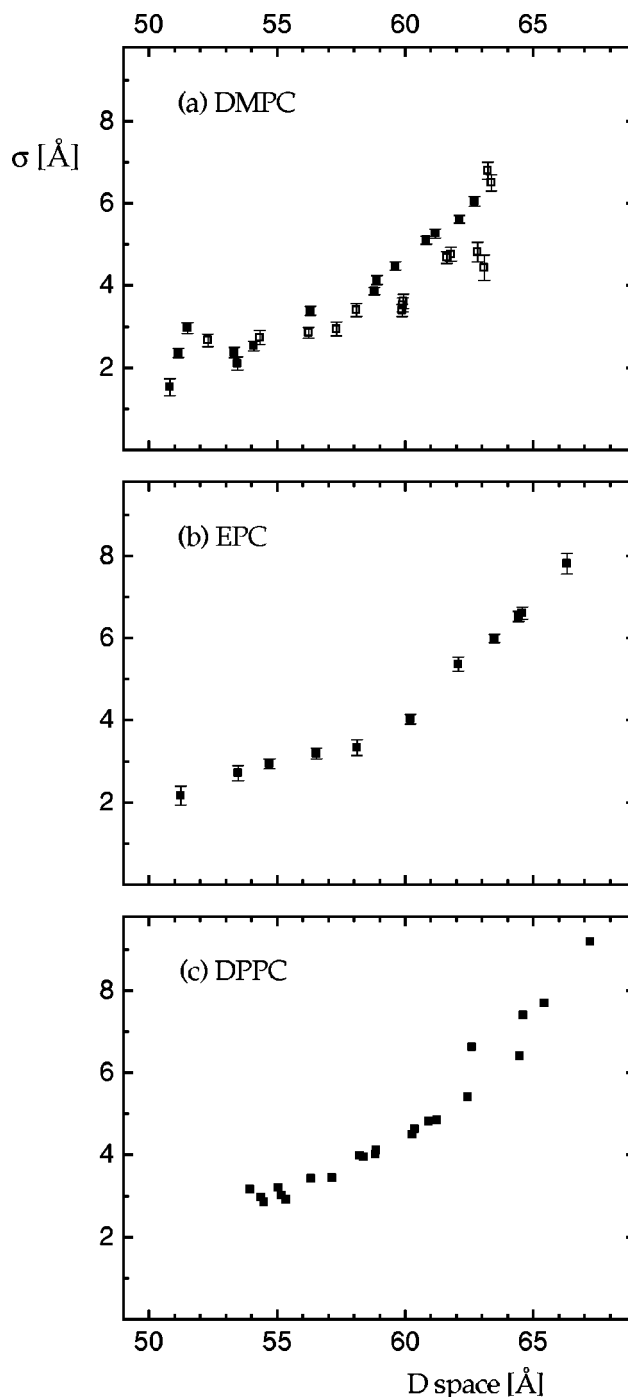


FIG. 4. Root mean square fluctuation  $\sigma$  vs  $D$  with same symbols and lipids as in Fig. 2.

osmotic pressure has little effect on volume  $V$  per lipid [32] and  $V=AD_B/2$ , this means that  $D'_B$  becomes larger with increasing  $P$ . The accepted way to calculate the change in  $A$  uses [7,33]

$$A - A_0 = -A_0 D_w P / K_A, \quad (27)$$

where  $K_A$  is the area compressibility that has been measured for DMPC to be 141 dyn/cm [33] in compression and 145 dyn/cm [22] in dilation. In our earlier paper [26] on DPPC we argued that  $A$  did not change upon increasing  $P$  from 0 to 24 atm. In retrospect, we find it noteworthy that

TABLE I. Parameters obtained from x-ray data for three lipids. All units are Å.

Lipid	$X_{HH}$	$D'_B$	$a_o$	$\lambda_{fl}$
DMPC	36.4	44.0	18.7	5.1
EPC	37.8	45.4	20.9	5.9
DPPC	39.6	47.2	20.0/19.0	6.0

our method that used only the highest  $P$  data gave  $A = 61.2 \text{ \AA}^2$  whereas our method that used all data from 0 to 24 atm gave  $A = 64.2 \text{ \AA}^2$ ; the sign of this difference is what one expects from the compressibility, although the magnitude of the difference is twice what one obtains from Eq. (27). We now believe that a systematic change in  $A$  and  $D'_B$  should be expected with increasing  $P$  and that this should be taken into account in obtaining  $a$ , especially since some of our new data go as high as 58 atm. For this highest  $P$  for DMPC, bilayer compressibility reduces  $a$  by 1.0 Å. Unfortunately,  $K_A$  has not been measured for DPPC or for EPC. For these lipids we have scaled  $K_A$  linearly with hydrocarbon thickness  $D_C$  compared to DMPC to obtain estimates of 150 dyn/cm for EPC and 160 dyn/cm for DPPC.

#### IV. FUNCTIONAL FORM OF $F_{fl}$

Inspired by Eq. (25) and Eq. (4) we plot  $\ln\sigma^{-2}$  versus  $a$  in Fig. 5. The results for all three lipids are consistent with  $F_{fl}$  following an exponential decay with decay lengths, defined as  $\lambda_{fl}$ , whose values are given in Table I. We note that if the compressibility correction to  $a$  had not been made, then the plots are also consistent with an exponential decay of  $F_{fl}$ , but with decay lengths about 0.2 Å shorter. Both sets of decay lengths are systematically greater than predicted by Eq. (4) as will become apparent when values of the hydration force decay constant  $\lambda$  are obtained.

The dashed curves in Fig. 5 show the prediction for hard confinement as embodied by Eq. (3); they simply use the basic hard confinement relation

$$(\sigma/a)^2 = \mu, \quad (28)$$

where  $\mu$  is a constant. The value of  $\mu$  has been given as 1/6 [16], 0.183 [15], and 1/4 [34]; the value 1/6 is used in Fig. 5. Comparing to the data shows first that hard confinement predicts a significant curvature in Fig. 5 that is not observed; in other words, the functional form of the undulation repulsion is incorrect. Second, the dashed curve lies below the data; raising it would require smaller values of  $\mu$  of order 0.05, but these values would also have to vary with  $a$ . From this comparison we conclude that a theory of soft confinement, such as the one given by Eq. (4), is required for the range of  $a$  in our data [35].

#### V. DECOMPOSITION OF $P(a)$ DATA

If we know  $K_c$ , then Eq. (26) can be used to determine  $P_{fl}$ . Unfortunately, literature values of  $K_c$  are either absent for some lipids or are uncertain by factors of 4 for other lipids, so we first tried using  $K_c$  as a fitting parameter along with the other parameters  $\lambda$ ,  $P_h$  and  $H$  in Eq. (1) using a

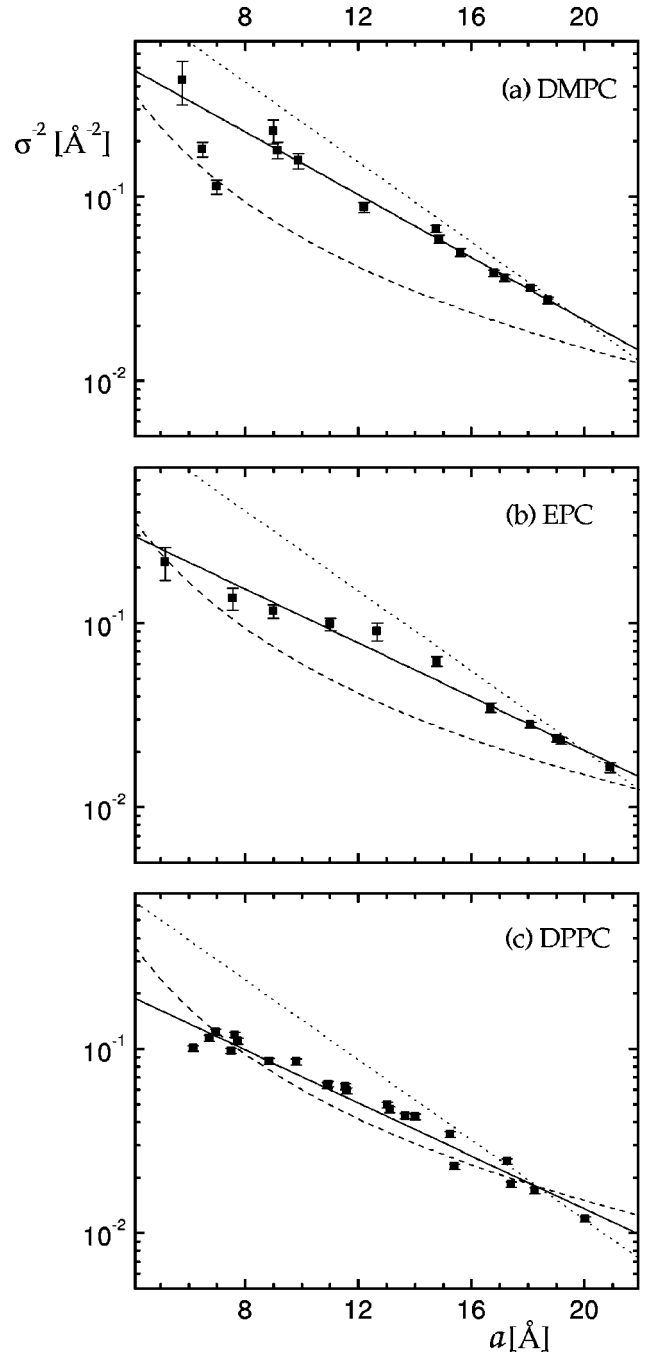


FIG. 5.  $\log\sigma^{-2}$  vs  $a$  for (a) DMPC, (b) EPC, and (c) DPPC. Only the most recent data are shown in (a) for DMPC. The solid lines show exponential fits. The dashed lines show the hard confinement prediction, Eq. (3), and the dotted lines show the slope for the soft-confinement prediction, Eq. (4).

routine nonlinear least squares program. For EPC the resulting parameters for this unconstrained fit are shown in line 1 of Table II. Figure 6(a) shows the fit to the  $\ln P$  data and also the decomposition into the three component pressures. However, by holding  $K_c$  fixed at other values, quite reasonable fits to the  $\ln P$  data can also be obtained as shown in Fig. 6(b). The results for the corresponding values of the other parameters, while holding  $K_c = 1 \times 10^{-12}$  erg and  $2 \times 10^{-12}$  erg, are shown in lines 2 and 3, respectively, in Table II.

Some fits for DMPC and DPPC are shown in Fig. 7. Fit-

TABLE II. Parameter values for several fits to  $\ln P$  data. The units are  $K_c(10^{-12} \text{ erg})$ ;  $P_h(10^9 \text{ erg/cm}^3)$ ;  $H(10^{-14} \text{ erg})$ , and  $\lambda$ ,  $a_0$ , and  $\Delta a_0$  are in  $\text{\AA}$ .

Lipid	$K_c$	$P_h$	$\lambda$	$H$	$a_0^{\text{fit}}$	$\Delta a_0$
EPC	0.55	1.07	1.94	4.73	20.9	7.4
	1.00	0.91	1.99	2.81	21.0	5.6
	2.00	0.81	2.03	1.65	21.0	3.7
DMPC	0.50	1.32	1.91	7.13	18.8	6.3
	0.80	1.13	1.97	4.91	18.8	5.0
	1.30	1.01	2.01	3.50	18.9	3.7
DPPC	0.50	0.63	2.36	9.19	16.0	2.3
	1.00	0.58	2.39	7.41	16.0	1.3
	0.50	0.99	1.97	4.78	18.0	4.5
	1.00	0.92	1.97	2.87	18.1	3.1

ting results for several fixed values of  $K_c$  for both lipids are shown in Table II. DPPC is more complicated because there is a wider range of  $a_0$  and the earlier data have larger uncertainties in  $P$ ; we therefore give results for the two extreme values of  $a_0$ .

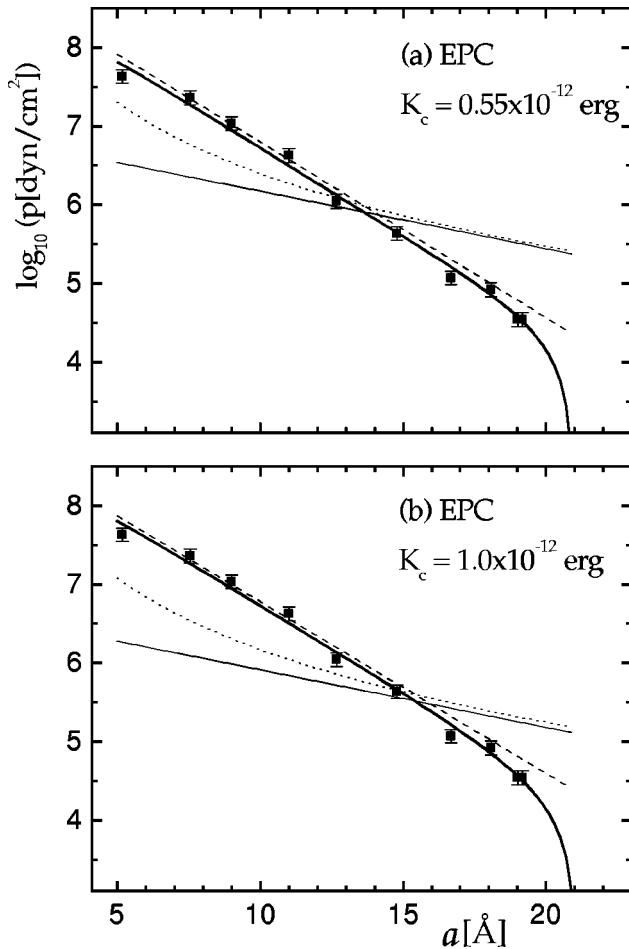


FIG. 6. The curved solid line shows the fit to  $\log(\text{osmotic pressure})$  vs  $a$  for EPC for the two values of  $K_c$  shown in (a) and (b). The straight solid line in each panel shows the fluctuation pressure, the straight dashed line shows the hydration pressure, and the curved dotted line shows the van der Waals pressure. Parameter values are given in Table II.

It is clear from the previous paragraph that additional information is required to determine the fitting parameters uniquely. One possibility is to hypothesize that the values of some of the parameters might vary little from lipid to lipid. For example, if the hydration pressure depends primarily upon water, then  $\lambda$  should be nearly the same for the three lipids. Also, the Hamaker parameter  $H$  might reasonably be expected to be nearly the same; the thickness dependence of the different bilayers is already accounted for in first ap-

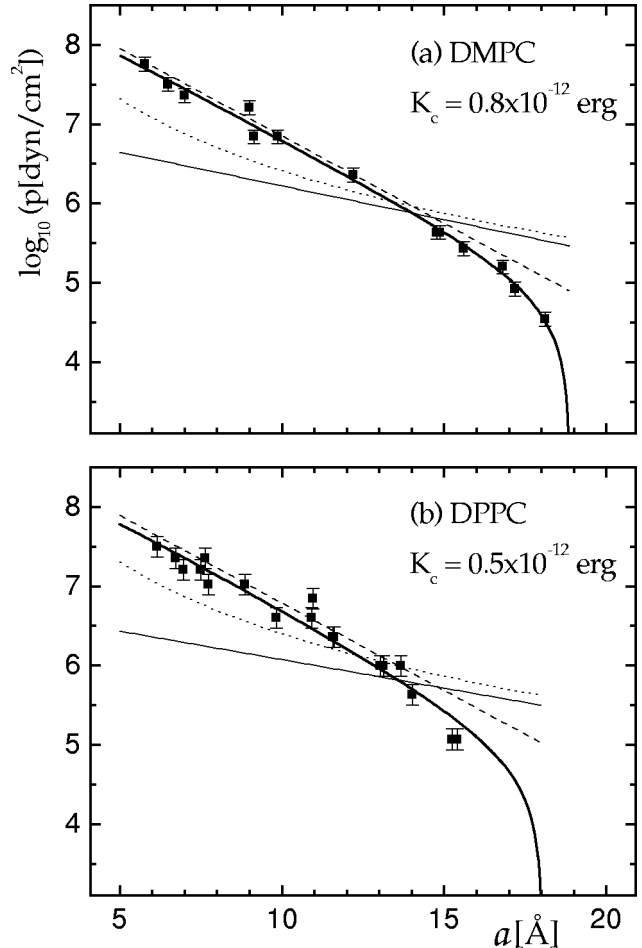


FIG. 7. As in Fig. 6 except that panel (a) is for DMPC and panel (b) is for DPPC.

proximation by the form of Eq. (2) and the relative proportion of head to tail does not vary much for these three lipids. These considerations disfavor the first two fits for DPPC listed in Table II, which were driven by the smallest estimate of  $a_0$ . From the last two fits we then conclude that  $\lambda$  is nearly 2.0 Å and  $P_h$  is about  $10^9$  ergs/cm<sup>3</sup>. These values of  $\lambda$  are only about 0.1 Å smaller than given by Rand and Parsegian [7]. The robustness of these values for  $\lambda$  and  $P_h$  follows from the fact that they are primarily determined by the high  $P$  data where the other two pressures are small as shown in Figs. 6 and 7. Because we make a compressibility correction, our  $\lambda$  are larger than those given by McIntosh and Simon [12]; if we did not make this correction our  $\lambda$  would be of order 1.8 Å.

Figures 6 and 7 show that the magnitude of the van der Waals pressure and the fluctuation pressure follow each other as  $K_c$  is varied, so the value  $H$  is no better determined than the value of  $K_c$ . There is, however, another criterion that can be used to establish preferences. Let us suppose that the hydration pressure and the van der Waals pressure are the same in the gel phase as in the  $L_\alpha$  phase, and that the fluctuation pressure is negligible because gel phase bilayers should be stiffer with larger  $K_c$ . Then,  $a_0$  in the gel phase would be the value of  $a$  at which the hydration pressure and the magnitude of the van der Waals pressure become equal; let us call this  $a_0^*$ . The difference  $\Delta a_0 = a_0 - a_0^*$  is given in Table II for the various fits. The experimental difference in  $a_0$  between  $L_\alpha$  and gel phase DPPC is 9 Å [26]. This favors the larger values of  $\Delta a_0$  in the last column of Table II, i.e., smaller values of  $K_c$  and larger values of  $H$ . However, when we consider even smaller values of  $K_c$  than given in Table II, the fit to the  $\ln P$  data deteriorates rapidly. The fact that the fitted values of  $\Delta a_0$  are smaller than 9 Å may, of course, reflect different values of some of the parameters for the gel phase. A similar criterion comes from oriented multilayers on solid substrates. Our most fully hydrated samples of DMPC [36] only have  $D$  spacings of 52 Å. Current theory [37] for these much smaller  $D$  spacings is that the substrate suppresses the fluctuations and this eliminates the fluctuational pressure. Since this should not change the other interactions or the bilayer thickness, one would have  $a_0^* = 52$  Å  $- 44$  Å = 8 Å, which would give  $\Delta a_0 = 11$  Å. One concern in the precise numerical value obtained from this criterion is that it is very hard to achieve 100% relative humidity for samples oriented on solid substrates; achieving higher humidity would, of course, reduce  $\Delta a_0$ .

Another criterion that one might use across the three lipids is to suppose that  $K_c$  might be larger for larger bilayer thickness. However, this criterion is weakened because EPC has unsaturated bonds that make the hydrocarbon chains more disordered than with saturated chains and the DPPC data were taken at higher temperature where the bilayer should be more flexible. Indeed, data taken at different temperatures (to be published) show that  $\sigma$  increases with temperature for DMPC and EPC. We therefore ignore this criterion in favor of the others above.

Since our best fit to EPC gives  $K_c = 0.55 \times 10^{-12}$  erg and since a similar value was obtained by direct measurement [17], we will choose line 1 in Table II. Assuming that the corresponding value of  $H$  should be nearly the same for all

three lipids leads us to suggest that  $K_c$  is about  $0.50 \times 10^{-12}$  erg for DPPC at 50 °C and  $0.80 \times 10^{-12}$  erg for DMPC at 30 °C. We note that the latter value is closer to the most recently measured value of  $K_c$  for DMPC at 25 °C than to the value measured at 30 °C [38].

## VI. B MODULI

In this section we address the rather confusing issue of various compression moduli that can be defined. The modulus  $B$  defined in the potential in Eq. (6) is related to  $\sigma$  by Eq. (19). It is important to appreciate that this  $B$  is a phenomenological input parameter; as such, it should not be expected to be equal to the thermodynamic output modulus  $B_T$ . Indeed, imposing such an equality would ensure that the bending term in Eq. (6) would have no effect in determining  $B_T$ . There are several ways that one can define the thermodynamic bulk modulus. The most straightforward is as  $-D(\partial P/\partial D)_T$ . It is more convenient, however, to consider  $-D(\partial P/\partial a)_T$ . Due to the compressibility of the bilayer these two ways are not the same, but the difference is less than 6% at our highest osmotic pressure.

Using either definition, we must also divide by  $D$  as was done in converting  $B_3$  in Eq. (5) to  $B$  in Eq. (6). We therefore define the thermodynamic modulus as

$$B_T = -\frac{\partial P}{\partial a}. \quad (29)$$

It is also useful to define a bare modulus

$$B_b = \frac{d^2 V(a)}{da^2} \quad (30)$$

and a fluctuating modulus

$$B_{fl} = \frac{d^2 F_{fl}(a)}{da^2}. \quad (31)$$

From Eq. (24) it then follows that

$$B_T = B_{fl} + B_b. \quad (32)$$

Figure 8 shows these four moduli obtained from our best fit to EPC. The bare modulus  $B_b$  is nearly equal to  $B_T$  for high  $P$  and small  $a$  because  $B_{fl}$  is relatively small. The relations change dramatically for larger  $a$  because  $B_b$  goes negative as  $a$  exceeds 17 Å; this is just a different statement of the fact that the fluctuation pressure swells  $a_0$  beyond  $a_0^*$ .

Most importantly, Fig. 8 emphasizes our assertion above that there is no general simple relation between  $B$  and any of the other three moduli. This is not surprising for general values of  $a$ . It is a somewhat surprising result in the limit of small values of  $a$ . In this limit one might expect that the effect of fluctuations would be negligible and that the hydration force would be dominant. Then, Eq. (22) suggests that  $B$  should equal  $B_b$ . If we imposed this constraint on the parameters,  $K_c$  would be reduced to about  $0.1 \times 10^{-12}$  erg and  $H$  would increase to over  $20 \times 10^{-14}$  erg; these values are clearly outside the currently acceptable range [13,17,38]. However, this constraint may not be appropriate because of

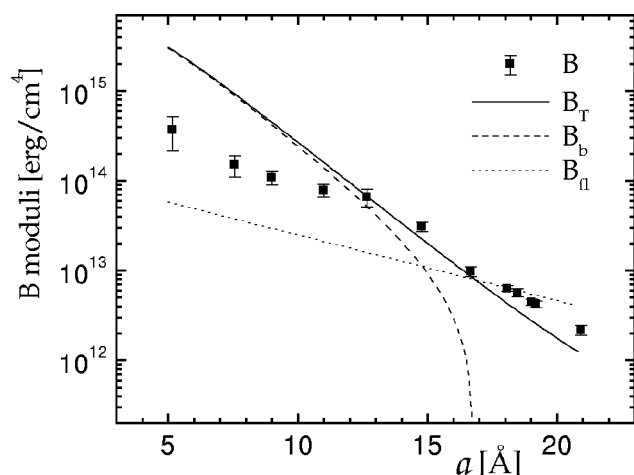


FIG. 8. log of various moduli as a function of  $a$ . Parametric modulus  $B$  (solid squares from  $\sigma$  data); thermodynamic modulus  $B_T$  (solid curve); bare modulus  $B_b$  (dashed curve, when positive) and fluctuating modulus  $B_{fl}$  (dotted line).

the harmonic approximation in Eq. (22) and also because our smallest values of  $a$  may not yet be in the small  $a$  regime.

## VII. CONCLUSIONS

Our  $\sigma$  data, presented in Sec. III, open a second window on interbilayer interactions, as we have shown theoretically in Sec. II, especially regarding the fluctuation pressure, for which our results are shown in Sec. IV. Our data show that a theory of soft confinement is definitely required for biological lipid bilayers, in contrast to some soft condensed matter systems [39] that were shown to obey Helfrich's theory of hard confinement. While the data support an exponentially decaying form for the fluctuation pressure, they have a decay

length  $\lambda_{fl}$  that is greater than twice the decay length  $\lambda$  of the hydration force predicted by the best theory of soft confinement [15].

Using this extended probe of the fluctuation force, we have then attempted to decompose the usual osmotic pressure data into component pressures without using additional information, such as the factor of  $K_c^{-1}$  in the fluctuation pressure. Ironically, the interaction that is the least well understood conceptually, the hydration pressure, is the one that can be best determined. In this regard, it is worth noting that other researchers have gone to much higher osmotic pressures [7,12]. Because the hydration pressure is already well determined with the range of pressures we use, we have concentrated instead on obtaining more data in the lower pressure range near full hydration where the other interactions play larger roles. One conclusion of our study is that the ability to fit the data, even with the new constraint on the functional form of  $P_{fl}$ , indicates that the functional forms of the hydration pressure and the van der Waals interaction in Eq. (1) remain acceptable, though perhaps not proven.

Furthermore, as we show in Sec. V, if either  $K_c$  or the Hamaker parameter  $H$  can be obtained from other experiments, then the remaining parameters can be extracted. It is indeed encouraging that choosing an experimental value of  $K_c$  [17,38] returns a reasonable value of  $H$  [13] and *vice versa*. Nevertheless, we regard this study as being a stepping stone to further study rather than as providing final answers to interbilayer interactions.

## ACKNOWLEDGMENTS

This research was supported by the National Institutes of Health Grant No. GM44976 to J.F.N. Synchrotron beam time was provided by CHESS under Project No. P727.

- 
- [1] E. A. Evans and V. A. Parsegian, *Ann. (N.Y.) Acad. Sci.* **416**, 13 (1983).
- [2] C. R. Worthington, *Biophys. J.* **9**, 222 (1969).
- [3] J. M. Anderson, *Annu. Rev. Plant Physiol.* **37**, 93 (1986).
- [4] G. S. Smith, C. R. Safinya, D. Roux, and N. A. Clark, *Mol. Cryst. Liq. Cryst.* **144**, 235 (1987).
- [5] J. N. Israelachvili, *Intermolecular and Surface Forces* (Academic Press, London, 1985), p. 149.
- [6] All experiments on unoriented multilamellar vesicles, such as those used for the data reported in this paper, obtain finite values of  $D_0$ . However, experiments of Harbich and Helfrich, [*J. Phys. (France)* **51**, 1027 (1990)]; on samples composed of oriented planar arrays do not obtain finite limiting values of  $D_0$  but instead obtain complete unbinding [S. Leibler and R. Lipowsky, *Phys. Rev. B* **35**, 7004 (1987)] for fully hydrated samples. This intriguing discrepancy will not be resolved in this paper.
- [7] R. P. Rand and V. A. Parsegian, *Biochim. Biophys. Acta* **988**, 351 (1989).
- [8] S. Leikin, V. A. Parsegian, D. C. Rau, and R. P. Rand, *Annu. Rev. Phys. Chem.* **44**, 369 (1993).
- [9] S. Marcelja and N. Radic, *Chem. Phys. Lett.* **42**, 129 (1976).
- [10] J. N. Israelachvili and H. Wennerstrom, *Langmuir* **6**, 873 (1990).
- [11] V. A. Parsegian and R. P. Rand, *Langmuir* **7**, 1299 (1991).
- [12] T. J. McIntosh and S. A. Simon, *Biochemistry* **32**, 8374 (1993).
- [13] V. A. Parsegian, *Langmuir* **9**, 3625 (1993).
- [14] T. J. McIntosh, A. D. Magid, and S. A. Simon, *Biochemistry* **26**, 7325 (1987).
- [15] R. Podgornik and V. A. Parsegian, *Langmuir* **8**, 557 (1992).
- [16] W. Helfrich, *Z. Naturforsch. A* **33a**, 305 (1978).
- [17] J. F. Faucon, M. D. Mitov, P. Meleard, I. Bivas, and P. Bothorel, *J. Phys. (France)* **50**, 2389 (1989).
- [18] E. A. Evans and W. Rawicz, *Phys. Rev. Lett.* **64**, 2094 (1990).
- [19] M. Kummrow and W. Helfrich, *Phys. Rev. A* **44**, 8356 (1991).
- [20] M. B. Schneider, J. T. Jenkins, and W. W. Webb, *Biophys. J.* **45**, 891 (1984).
- [21] D. Sornette and N. Ostrowsky, *J. Chem. Phys.* **84**, 4062 (1986).
- [22] E. A. Evans and D. Needham, *J. Phys. Chem.* **91**, 4219 (1987).
- [23] R. Zhang, R. M. Suter, and J. F. Nagle, *Phys. Rev. E* **50**, 5047 (1994).
- [24] A. Caille, *C. R. Seances Acad. Sci., Ser. B* **174**, 891 (1972).

- [25] P. G. DeGennes, *J. Phys. (Paris), Colloq.* **30**, C4-65 (1969).
- [26] J. F. Nagle, R. Zhang, S. Tristram-Nagle, W. Sun, H. I. Petrache, and R. M. Suter, *Biophys. J.* **70**, 1419 (1996).
- [27] R. Zhang, S. Tristram-Nagle, R. L. Headrick, T. C. Irving, R. M. Suter, and J. F. Nagle, *Biophys. J.* **70**, 349 (1996).
- [28] R. Holyst, *Phys. Rev. A* **44**, 3692 (1991).
- [29] N. Lei, C. R. Safinya, and R. F. Bruinsma, *J. Phys. II* **5**, 1155 (1995).
- [30] T. J. McIntosh and S. A. Simon, *Biochemistry* **25**, 4058 (1986).
- [31] J. F. Nagle, *Biophys. J.* **64**, 1476 (1993).
- [32] S. H. White, R. E. Jacobs, and G. I. King, *Biophys. J.* **52**, 663 (1987).
- [33] B. W. Koenig, H. H. Strey, and K. Gawrisch, *Biophys. J.* **73**, 1954 (1997).
- [34] W. Janke and H. Kleinert, *Phys. Lett. A* **117**, 353 (1986).
- [35] If  $a$  were much larger than in our bilayers, then one would expect the functional form to approach the hard confinement curve. Of course, this is a moot point because  $a$  is limited by the full hydration value  $a_0$ .
- [36] S. Tristram-Nagle, H. I. Petrache, R. M. Suter, and J. F. Nagle, *Biophys. J.* **74**, 1421 (1998).
- [37] R. Podgornik and V. A. Parsegian, *Biophys. J.* **72**, 942 (1997).
- [38] P. Meleard, C. Gerbeaud, T. Pott, L. Fernandez-Puente, I. Bivas, M. D. Mitov, J. Dufourcq, and P. Bothorel, *Biophys. J.* **72**, 2616 (1997).
- [39] C. R. Safinya, E. B. Sirota, D. Roux, and G. S. Smith, *Phys. Rev. Lett.* **62**, 1134 (1989).